

# Leaking gas from a snow-covered pipe: empirical evidence and modeling of preferential flow paths

**Robert W Ashcraft, Alfonso Ibarreta and Timothy J Myers**

Exponent, Inc., 9 Strathmore Rd., Natick, MA 01760, USA

## Abstract

The potential dangers associated with exposed fuel gas pipes in areas of significant snowfall are examined. There have been numerous incidents in the past two decades where snow loading or impact on fuel gas equipment has been identified as one step in the sequence of events leading to fires or explosions. This study experimentally and numerically examines the possibility of snow cover creating a preferential pathway for gas flow into a nearby structure from a leaking pipe. Simple experiments show that when a suspended pipe is covered with snow, a gap often forms directly underneath the pipe, which has the potential to serve as a low-resistance flow path for fugitive fuel gas. Using a simplified geometry, the fraction of gas entering a nearby structure from a leaking, snow-covered pipe is examined using finite differences to solve the flow equations in porous media. The snow cover is shown to force a large portion of the fugitive gas toward the structure under certain circumstances and has the potential to create additional hazards that would not be present without the snow layer. Using sensitivity analysis, the major parameters governing fugitive gas flow are determined, which include internal structure pressure, gap size, snow permeability, and distance of the leak from the structure.

## Keywords

Explosion, snow, porous media, propane, fuel gas, fire, safety, risk assessment

---

## Corresponding author:

Robert W Ashcraft, Laboratory for Chemical Technology, Ghent University, Krijgslaan 281, Building S5, 9000 Ghent, Belgium

Email: [rwashcra@gmail.com](mailto:rwashcra@gmail.com)

## Introduction

Propane and natural gas are common fuels used in heating systems and appliances in residential and commercial structures throughout the country. House explosions in the northern and mountainous regions of North America have been attributed to fugitive fuel gas from snow-covered outdoor leaks accumulating in a structure and being ignited. In some regions, this introduces a possible failure mode not present in more temperate climates: damage from accumulated or falling snow and ice and the creation of a preferential flow path to the structure. The National Fire Protection Association has identified protection from snow and ice as an important safety precaution in areas of heavy snowfall. In response to a series of incidents in the Sierra Nevada Mountains in 1993, NFPA 58 [1] added snow-related requirements including: 'In areas where heavy snowfall is anticipated, piping, regulators, meters, and other equipments installed in the piping system shall be protected from the forces anticipated as a result of accumulated snow.' Typically, the above-ground portion of the gas piping involves short spans of pipe that are less susceptible to damage from snow loads. However, in some installations long spans of above-ground piping are found that are more susceptible to failure if not adequately protected.

The flow of fugitive gas through porous media is also of concern with underground natural gas piping. Sometimes loosely packed or coarse media are used to fill in the pipe trench prior to a top layer of dirt resulting in higher permeability region near the pipe, surrounded by a lower permeability region composed of natural soil. If a pipe leak occurs, the fugitive gas can preferentially travel significant distances in the highly permeable region around the pipe rather than through the soil to the surface where the gas is dispersed into the air. The fugitive gas can then access structures through dormant piping or other unintended conduits to create flammable fuel/air mixtures within the structure. Although the study here does not directly address this situation, the analysis can be generalized to predict the behavior of layers of different permeabilities.

There have been 29 explosions and/or fire incidents identified in the past two decades in the USA where the cause was attributed to snow loads or impacts fracturing fuel gas piping or equipment near a structure.<sup>a</sup> Of these incidents, 75% have occurred within the last 10 years. The geographic locations of reports of this type are generally clustered in areas where large amounts of snowfall are common. Two events occurred in the Cascade Mountains in Washington and Oregon, six occurred in the Sierra Nevada Mountains in California, eight occurred in the Rocky Mountains in Wyoming, Utah, and Colorado, nine occurred in the Green and White Mountains in Vermont and New Hampshire, three occurred in areas where lake-effect snow is prominent in Michigan and New York, and one event occurred in eastern Pennsylvania. A greater number of incidents have been identified in more recent years most likely due to the digitization of records and the increased accessibility and dissemination of information provided by the internet.

The hazard is that many above-ground sections of a fuel piping network are close to the structure to which fuel is being supplied. Often, the piping, regulator,

and/or metering devices are located under eaves of the roof to provide 'protection,' where in reality snow and ice accumulated on the structure's roof has the greatest tendency to fall and cause damage in these locations. A document from the US Army Corp of Engineers highlights the potentially damaging consequences of snow and ice falling from buildings, including several images of damage [2]. There is the potential for falling masses of snow and ice to impact above-ground piping and equipment with enough force to cause breaches in the system, resulting in the release of fugitive gas. Normally, a leak in the low-pressure portion of an above-ground gas system that is located away from openings to a structure will disperse and be diluted by outdoor air, and gas will not enter the structure in significant quantities. However, gas from a snow-covered leak may be able to migrate into the building through preferential flow paths such as gaps around the gas pipe, high-permeability regions in the snow, cavities near the building, through openings in the building, or through permeability of building materials. One such flow path can be created by gaps close to the wall of the pipe that can cause fuel gases to be preferentially directed toward the structure. If the structure has gaps at the pipe entry point or other potential entry points under the snow line, then the fugitive fuel gas may be able to infiltrate the structure at a rate large enough to overcome the lower flammable limit within a portion of the structure. In some of the incidents reviewed, it was reported that gas migrated along gaps around pipes. In another case, gas from a leak near a propane tank migrated to another building that was not supplied with gas. These phenomena are also well known to occur from leaks in underground gas pipes [3,4]. Leaks underground or under snow will follow the path of least resistance whether it is flowing through high-permeability regions of earth or snow, along gaps around pipes, or through abandoned pipes. In some cases, wind can significantly influence the pressure condition at the snow surface and affect flow patterns within the snow layer [5,6]. Empirical evidence and modeling results supporting the idea that fugitive gas can propagate preferentially along a pipe buried within the snow layer will be presented in this article.

## Experimental studies

Two simple experiments were carried out to examine the presence of a void space below pipes buried in snow. In the first test, two empty, capped pipes were mounted 305 mm above the ground, and snow was allowed to naturally deposit around them. The pipes had outer diameters of 21.3 mm (0.84 in.; '½-in.' iron pipe) and 33.5 mm (1.32 in.; '1-in.' iron pipe), each approximately 1.8 m long. The center span of the pipe between supports measured approximately 1.2 m. In the second test, loose snow was shoveled on top of the elevated pipes in an attempt to mimic the effect of snow falling off a roof onto the pipe and covering it. This was not an attempt to cause damage to the pipe. After covering the pipes, the snow was allowed to settle for 3 days, and then the pipes were excavated to document the condition and geometry of the snow around the piping.

### Test 1 – accumulated snow

The accumulated snow test was performed in Sterling, MA, USA between January 28 and 29, 2009. The snow storm on January 28 deposited approximately 100 mm of snow on top of a pre-existing layer of snow approximately 180 mm deep. The snow was followed by approximately 19 mm of sleet and freezing rain, leaving a denser top layer of accumulation. The result of the precipitation was a partially covered ‘1-in.’ pipe and a nearly covered ‘½-in.’ pipe. The bottom of the pipes generally resided near the snow/sleet interface. The density of the bulk snow layer and the bulk ice layer was measured by excavating a known volume of snow or ice, and weighing the resulting sample. The density of the snow was calculated to be  $130 \text{ kg/m}^3$  with an estimated error of  $\pm 15 \text{ kg/m}^3$ . The density of a sample of the top sleet/ice layer was calculated to be  $620 \text{ kg/m}^3$ .

Each pipe was excavated the morning after the snowfall to determine the size and shape of gaps. The temperatures were below freezing throughout the excavation, and there was no evidence of melting. The ‘1-in.’ pipe was analyzed first, and an approximately 5–10 mm gap was observed underneath the pipe, as shown in Figure 1(a). A clear gap is present in the area where the pipe was only partially covered, either from the pipe acting as a shield and preventing accumulation underneath it or from settling of the snow/sleet after deposition. The ‘½-inch’ pipe was examined next, and showed very similar results. The entire pipe was covered with the icy layer, and the bottom of the pipe was not accessible without breaking the surface layer. An image from the excavation is shown in Figure 1(b), showing an approximately 5 mm gap below the pipe. The images also show the granular nature of the sleet-like layer on top of the snow. Again, clear evidence is seen of the formation of a gap that could provide a preferential pathway for gas flow along the length of the pipe. The formation of the gap underneath the pipe is believed to be due to settling of the snow and ice during and after the precipitation.

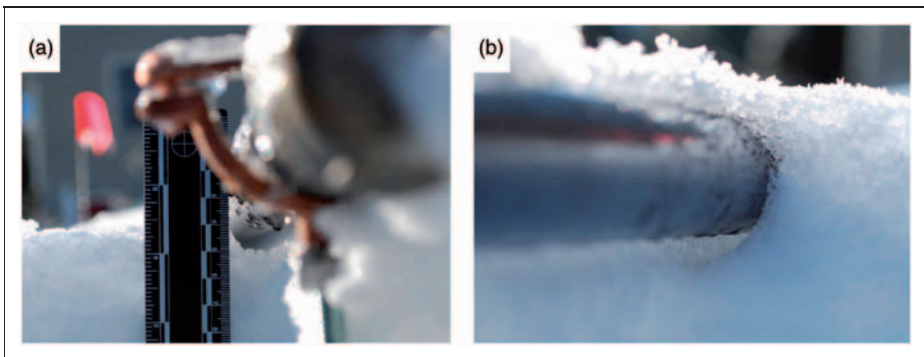


**Figure 1.** (a) Image of the ‘1-in.’ pipe showing gap formation underneath ( $\sim 10 \text{ mm}$ ); (b) image of the ‘½-in.’ pipe showing a gap under the fully covered portion of the pipe ( $\sim 5 \text{ mm}$ ).

The semicircular nature of the gap and the fact that the shape corresponds directly with the curvature of the bottom of the pipe in both cases are consistent with settling as the formation mechanism.

### *Test 2 – shoveled snow*

In the second test, fresh, loose snow was shoveled on top of the suspended pipes after a recent snow fall. This took place between March 4 and 8, 2009 in Hopkinton, MA, USA. The test was meant to roughly mimic the condition where loose, non-compacted snow would be falling from an elevated surface onto gas distribution equipment. After the snow was piled on top of the apparatus, the setup was left to ‘age’ for 3 days before initial excavation activities began. A brief photo-timeline of the events is shown in Figure 2, showing the post-snow, post-shoveling, and pre-excitation conditions of the test setup. The post-snow temperatures were above freezing, and it is clear that significant snow melting occurred during this time period. Due to the snowmelt, a portion at one end of the pipes was exposed to ambient conditions, as seen in the photo-timeline.

The excavation of the ‘1-in.’ pipe was performed at the end still completely covered with snow. The covered end of the pipe yields a more representative gap size, given that the other end of the pipe was exposed to the atmosphere for part of the aging time. Photographs of the observed gap are shown in Figure 3. The gap present in this scenario was observed to extend 15–20 mm below the pipe, noticeably larger than the gap in the naturally deposited snow test in which the pipe was excavated immediately after the snowfall. This implies that either aging or the method of snow deposition plays a role in the size of the void space underneath the pipe. In this test, a partial oval shaped gap was observed, with the bottom having the curvature of the pipe. This is a further evidence that settling of the snow is the mechanism of gap formation.

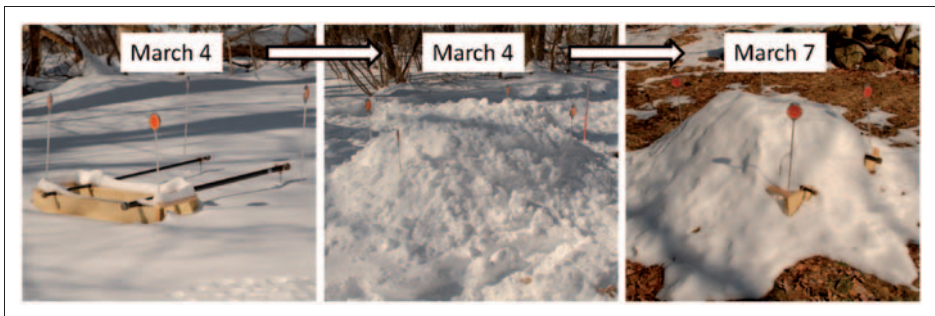


**Figure 2.** Progression in the shoveled-snow test over the course of 3 days, showing initial snow accumulation, condition after shoveling, and the pre-excitation condition 3 days later.

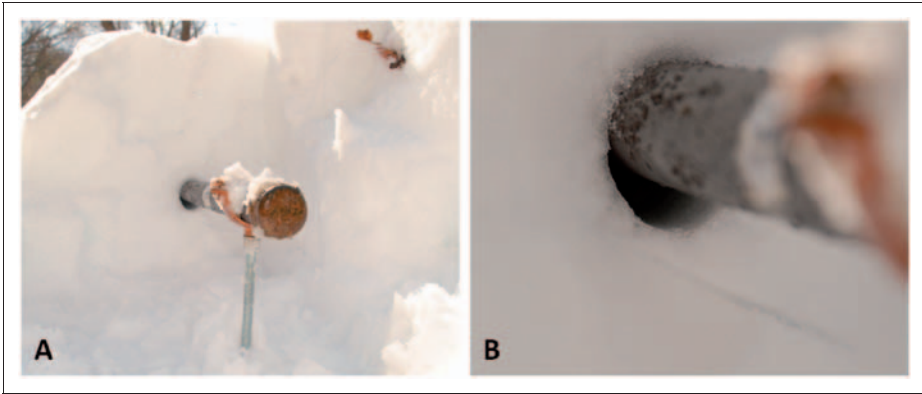


**Figure 3.** Images from the ‘1-in.’ pipe excavation in the shoveling test, showing the gap approximately 400 mm from the end of the pipe.

### *Experimental results and discussion*

In two different scenarios, evidence of gap formation underneath a suspended pipe was observed. The size of the gap varied with changes in pipe diameter, the conditions under which the snow was deposited, and with length of time before excavation. A gap extended below the ‘ $\frac{1}{2}$ -in.’ iron pipe measuring approximately 5 mm over the length of the pipe in the naturally deposited snow test. A gap extended below the ‘1-in.’ iron pipe and it measured 10–20 mm in the two tests. This is clear evidence that gap formation can and does occur underneath a pipe when covered in snow. The gap can then serve as a low-resistance pathway for gas flow, as compared with gas flow through the low permeability, porous structure of the surrounding snow.

The likely mechanism for gap formation is deposition of the snow followed by settling or densification of the snow. Settling can occur by at least two mechanisms: (1) gravitation forces acting on the particles (overburden), causing them to pack more tightly and the snow layer thickness to shrink, and (2) metamorphism/sintering processes whereby the snow particle morphology changes and the snow volume decreases. Both gravitational settling and shrinkage due to the initial stage of metamorphism involving fine structure elimination are very active in the hours to days after a fresh snowfall [7]. Various studies [8,9] have documented this process at subfreezing temperatures.

### **Modeling the migration of gas within the gap**

Once the presence of a gap was observed, the next question to address was how efficient the void would be in preferentially directing gas flow along the pipe. A simplified two-dimensional (2-D) system was chosen to approximate a realistic situation in which a leak may occur and the effect of different parameters could easily be compared. An axis-symmetric cylindrical system consisting of a straight

pipe surrounded by an annular gap and a shell of snow was used as the simplified geometry. An impenetrable wall is present on the left side of the domain (representing the gas pipe exiting the ground). A similar wall is present on the right side that mimics the wall of the structure, which has a structural gap allowing gas to exit the system into the structure. In addition to the wall gap, gas exits the system through the cylindrical snow shell. Gas enters the system through a ‘slice’ cut out of the pipe in the form of a radial jet. The region around a buried gas pipe mounted against a wall could be approximated by  $\frac{1}{2}$  of the cylindrical geometry. Similarly, the region around a buried gas pipe mounted near the intersection of the ground and a wall could be approximated by  $\frac{1}{4}$  of the cylindrical geometry.

The simplified geometry differs from more realistic scenarios. In an actual situation, the pipe would essentially be submerged in a slab of snow, with the (approximately) impermeable ground below and the ambient above. This model should be seen as a study of the important parameters which govern the partitioning of gas flow between the structure and dispersion in the air, rather than a model for a specific installation. The physical conditions of the snow, the geometry of the piping system, and the mechanism of a given system failure are all variables which are difficult to generalize. Therefore, a sensitivity study with a simplified system is a reasonable way to examine general trends.

### *Numerical technique*

In setting up the problem, axial symmetry was used in order to reduce the number of dimensions, the computation cost, and complexity. This allows for the use of finer resolution in the solution for a given physical size of the system. The 2-D domain, set up in cylindrical coordinates is shown in Figure 4, with many of the features enlarged and not-to-scale. The bottom edge of the domain corresponds to the pipe wall, and is a zero-flux boundary with the exception of the gap where the fugitive gas enters the system. This boundary is at a radius equal to  $R_{\text{pipe}}$ , with the width of the gas leak equal to  $w_{\text{leak}}$ . The boundary condition at the leak location is a fixed flux, based on the volumetric flow of the pure gas entering the system. The left-hand boundary is an impermeable wall with a zero-flux condition. An annular void space is present between the pipe wall and the start of the snow shell and extends from  $R_{\text{pipe}}$  to  $R_{\text{ann}}$ , for a total width of  $w_{\text{ann}}$ . The cylindrical snow shell extends from  $R_{\text{ann}}$  to  $R_{\text{snow}}$ , for a total thickness of  $w_{\text{snow}}$ . The top boundary of the system corresponds to the interface of the snow layer with the ambient, at a pressure equal to  $P_{\text{amb}}$ . The boundary condition here is an ambient pressure condition in which the relative pressure is set to zero at  $R_{\text{snow}}$ . The total length of the domain is  $L_{\text{total}}$ , and the distance from the structural boundary (right side) to the center of the leak is denoted  $L_{\text{leak}}$ . The right boundary is a composite of a no-flux wall and a fixed pressure gap region where gas can exit the system. The structural gap extends from the pipe wall a distance equal to  $w_{\text{gap}}$ , which can be set independently of the width of the annular region. The flow through the structural gap corresponds to gas flow into the structure, and the boundary condition at this location is the

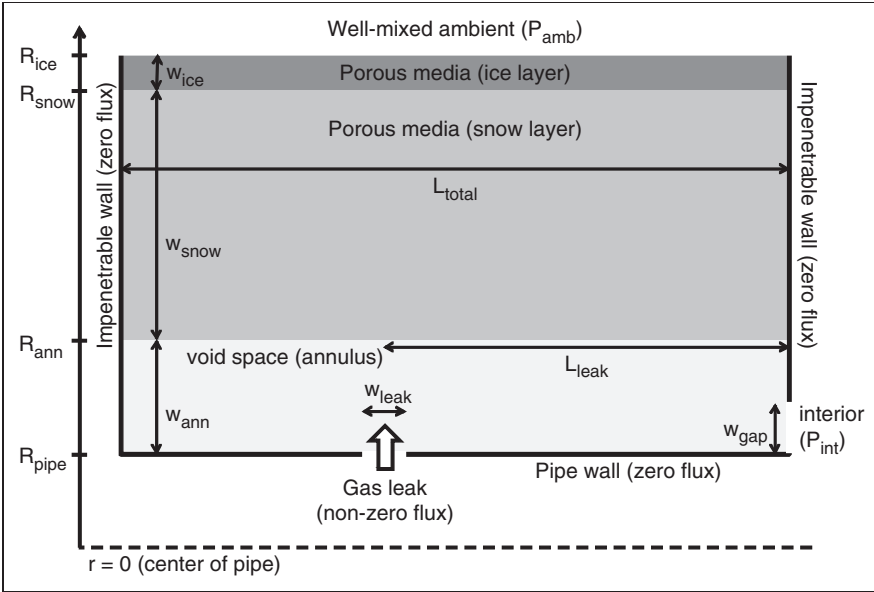


**Figure 4.** Not-to-scale representation of the solution domain of the problem, indicating the important geometric parameters present in system.

relative internal pressure of the structure,  $P_{int}$ , which may be below ambient pressure due to stack effects often present in structures in the colder months. An ice layer with a thickness  $w_{ice}$  is also shown in the figure, the effect of which will be examined in some of the analyses discussed later in the article (an ice layer is not present in the base model).

A combination of Darcy's law and the continuity equation was used to solve for the pressure and velocity profiles within the system under steady-state conditions. Under these conditions, the pressure will be directly related to the gas concentration, as nearly all gas within the system at steady state will be fugitive gas from the leak. Back diffusion of ambient species into the system was determined to be negligible and was not included in the numerical simulation. The differential equations were solved using the method of finite differences. Due to the highly disparate length scales involved in the problem, namely the size of the gap and leak relative to the snow layer and overall length, a non-uniform grid was used in both the radial and axial directions. This allows for fine resolution around the leak location and in the annular void space, where the velocities are higher. With the assumption of constant viscosity and permeability, the continuity equation and Darcy's law representation of the velocities can be combined to yield the governing equation in the bulk of the solution domain, as shown in Equation (1).

$$0 = \frac{1}{r} \frac{\partial}{\partial r} \left( r \cdot \frac{k}{\mu} \frac{\partial P}{\partial r} \right) + \frac{k}{\mu} \frac{\partial^2 P}{\partial z^2} \quad (1)$$



In these equations,  $k$  is the Darcy permeability of the medium through which the fluid is moving and  $\mu$  the viscosity of the fluid. A further simplification is that Darcy's law was also used in the annular gap around the pipe, which is clearly not porous media. The primary reason for utilizing Darcy's law in the gap region was to avoid the non-linearity that would be introduced had more rigorous equations such as the Navier–Stokes equations been used. However, the effective permeability value used in the gap region was calculated based upon the viscous solution to incompressible flow in an annular region, which will result in similar average axial velocities in the gap region when comparing the Darcy's law estimate and the viscous flow solution. For laminar flow, the effective Darcy permeability in the axial direction of the annular region can be defined by Equation (2) [10]:

$$k_{\text{eff}}^{\text{ann}} = \frac{\alpha \cdot R_o^2}{8}, \quad \text{where } \alpha \equiv \left[ \frac{1 - \kappa^4}{1 - \kappa^2} - \frac{1 - \kappa^2}{\ln\left(\frac{1}{\kappa}\right)} \right] \text{ and } \kappa \equiv \frac{R_i}{R_o} \quad (2)$$

Here  $R_i$  and  $R_o$  are the inner and outer radii of the annulus. For a 19-mm ( $\frac{3}{4}$  in.) outer diameter pipe with an inner annular radius of 9.5 mm, a 1.0 mm gap width would result in an effective permeability of  $8.3 \times 10^{-8} \text{ m}^2$ , and a 10 mm gap width would result in a value of  $8.4 \times 10^{-6} \text{ m}^2$ . These strictly correspond to axial-flow permeability values; however, the values were also used in the radial direction. The radial permeability of the gap has a negligible effect on calculations due to its low flow resistance relative to the radial flow resistance of the snow.

### Modeling results and discussion

In order to solve the system of equations defined above, several geometric, atmospheric, and physical property parameters need to be defined. These include the system pressures, gas viscosity, snow permeability, annulus size, snow layer thickness, structural gap size, overall length, leak flow rate, leak size, and leak location. The experimental results have provided a general range in which some of the parameters should exist, yet there is still a large amount of uncertainty due to natural variation in the snow cover, potential geometries, and the specifics of actual systems. For this reason, the analysis was focused on what is considered to be a plausible combination of parameters, with examination of the sensitivity of key outputs to variations in the model parameters. In general, the effect of simultaneously changing multiple parameters was not investigated due to the combinatorial nature of the problem, though in some cases, the effect of multiple parameters could be merged into a single curve.

The viscosity of propane at 273 K was used in the calculations and was determined to be  $7.7 \times 10^{-6} \text{ kg}/(\text{m}\cdot\text{s})$  [11]. The permeability of snow is more difficult to

determine and is highly dependent on the characteristics of the snow as deposited and the ambient conditions as the snow ages. Several authors [12,13] have examined the permeability of snow under various conditions. Shimizu [12] proposed a relationship between the permeability, grain size, and snow density, which was used to estimate a baseline permeability for the calculations. Based on the density and grain size ranges studied by Shimizu, the expression for permeability was evaluated with a density of  $300 \text{ kg/m}^3$  and a grain size of  $0.5 \text{ mm}$ . The resulting permeability was determined to be  $1.8 \times 10^{-9} \text{ m}^2$ , with a typical range for snow being approximately  $1 \times 10^{-10}$  to  $1 \times 10^{-8} \text{ m}^2$ . Field measurement [14] in northern Vermont in the 1992–1993 snow season revealed permeability values in the range  $3 \times 10^{-10}$  to  $7.5 \times 10^{-9} \text{ m}^2$ , in line with the value used in this analysis. Further measurements [15] in Vermont in the 1999–2000 determined snow layer permeability to be in the range from  $5 \times 10^{-9}$  to  $1 \times 10^{-8} \text{ m}^2$ , for a single measurement location. The width of the annular region was chosen to be  $5 \text{ mm}$  based on observations from the experimental snow studies discussed above. This parameter is clearly subject to variation and is included in a sensitivity analysis. The width of the structural gap was assumed to be  $2 \text{ mm}$  in the base scenario, irrespective of the size of the annulus. The overall length of the pipe was taken to be  $3 \text{ m}$ , and the location of the crack was taken to be  $1 \text{ m}$  from the structural boundary. The width of the crack was chosen to be  $4 \text{ mm}$ , though the crack size has little influence on the solution over the range of reasonable values. The relative ambient pressure and relative pressure inside the structure were both taken to be 0; the effect of a lower internal pressure, which can occur due to stack effects, was investigated in the sensitivity analysis. The outer pipe radius was taken to be  $9.53 \text{ mm}$  in all cases ( $0.75 \text{ inch}$  outer diameter).

**Base model results.** The results from the base model, as described in the previous section, were computed by solving the finite difference equations on a grid size of approximately  $400 \times 400$ . There were 201 grid points in the  $5 \text{ mm}$  annular region nearest the pipe in the radial direction ( $\Delta r = 0.025 \text{ mm}$ ) and 205 grid points in the  $1 \text{ m}$  thick snow region in the radial direction ( $\Delta r = 4.90 \text{ mm}$ ). There were 151 total points in the bulk regions before (101 points,  $\Delta z = 20 \text{ mm}$ ) and after (50 points,  $\Delta z = 20 \text{ mm}$ ) the crack in the axial direction, 150 points in the region surrounding the crack in the pipe ( $\Delta z = 0.067 \text{ mm}$ ) in the axial direction, and 100 points in the nearest  $20 \text{ mm}$  to the structural wall ( $\Delta z = 0.20 \text{ mm}$ ) in the axial direction. The grid points within each region were evenly spaced. Note that the above grid spacings are valid for the base model, and grid spacing changed when geometrical parameters (e.g., snow layer thickness and annular width) were varied during the parametric study. The dense portions of the grid in the annular and crack regions extend beyond the edge of either structure, to ensure more accurate depictions of the behaviors near the edges of these features.

The leak rate in all calculations was assumed to be approximately  $0.002 \text{ m}^3/\text{s}$  at  $273 \text{ K}$  ( $4.6 \text{ ft}^3/\text{min}$  at  $298 \text{ K}$ ) and  $101,325 \text{ Pa}$ . This is representative of the maximum flow rate from a second stage propane regulator that may be used on a home and corresponds to  $190 \text{ kW}$  ( $650,000 \text{ Btu/h}$ ) for propane gas.

The calculated pressure field in the system is shown in Figure 5, where the radial direction is plotted on a logarithmic scale to better resolve the annular region. The maximum pressure observed in the system was 5.1 Pa (0.02 in. of water) above the ambient pressure and occurred in the area closest to the leak, as would be expected. The radial pressure drop is essentially zero in the annular region, due mainly to its low flow resistance and thinness relative to the snow layer. Once in the snow region, the pressure drop is clearly evident due to the relatively low permeability and large width of the snow layer. The streamlines indicate, as expected, a portion of the gas travels directly from the crack to the structural gap through the annular void region. The distinctly curved streamlines between lengths of 2.75 and 3 m are created because low-pressure zones exist both above (at the snow surface) and below (at the structural gap). This allows for the flow bifurcation point near  $r=0.2$  m, where the flow paths diverge to their respective outlets. The low pressure in the annular region at a length of 3 m is due to the structure pressure boundary condition.

The velocity field is directly related to the pressure field *via* Darcy's law, and is dependent on the permeability of the media, the fluid viscosity, and the pressure gradient. The radial and axial velocities were calculated using finite difference-type equations and the appropriate permeability to where the velocity is being calculated. These velocities were integrated over the boundaries to calculate the flux and partitioning of fugitive gas between the system outlets.

The most important observation from these calculations is the partitioning of the fugitive gas between the ambient and the structure. To quantify how much gas

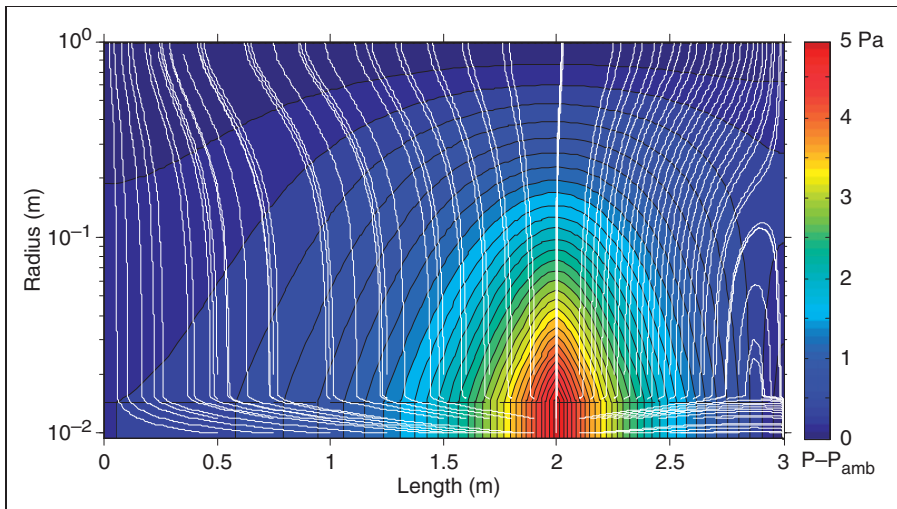


**Figure 5.** Calculated pressure field in the system.

Note: The dashed line corresponds to the annular gap boundary; the maximum pressure occurs near the crack and is approximately 5 Pa above the ambient pressure; flow streamlines are shown in white.

entered the structure, the percentage of the fugitive gas entering the structure was calculated. The closure of the total mass balance was monitored, and in all cases, the difference between the amount entering and exiting the system was less than 0.1% of the total flow. For the base case scenario, the total input to the system was 0.0907 mol/s, the flow out of the structure gap was 0.0156 mol/s, and the flow to the ambient through the snow surface was 0.0751 mol/s. The amount of flow into the structure was 17.1% of the total flow, with a mole balance discrepancy of 0.001%. The convergence of the model improved as the number of grid points increased.

**Sensitivity analysis.** The sensitivity of the model to the geometric and physical property parameters is important due to their natural variability. This section examines the change in the amount of gas exiting through the structural gap, as certain key parameters are changed individually. The first parameter that was probed was the effect of the snow radius. As the thickness of the snow increased, one expects that the resistance to flow will also increase, causing more of the gas to leave through the structural gap despite the large external surface area of the snow. As expected, the flow through the structural gap increases with the radius of the snow, with the flow rising approximately logarithmically. The dependence is shown in Figure 6(a) for snow permeabilities of  $1 \times 10^{-10}$ ,  $1.8 \times 10^{-9}$ , and  $1 \times 10^{-8} \text{ m}^2$ .

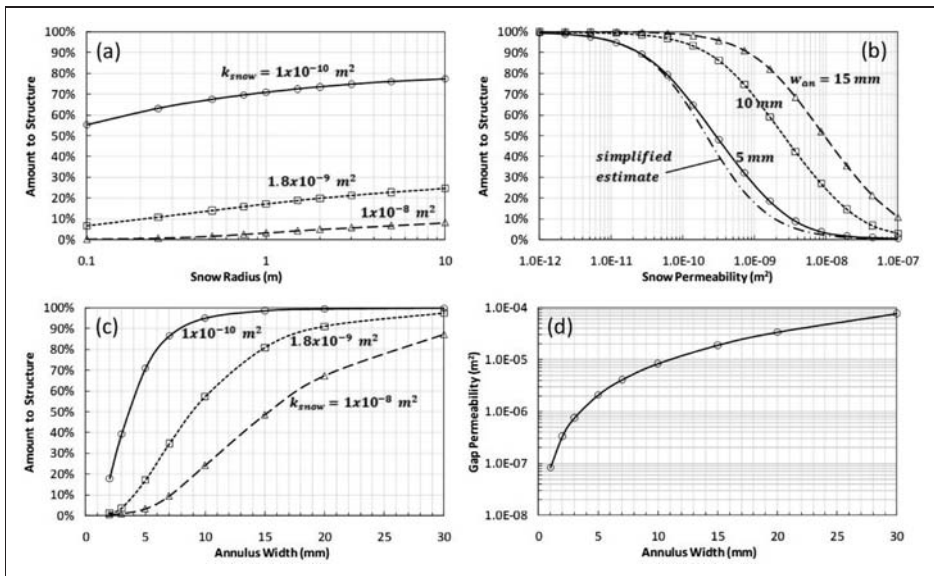


**Figure 6.** Sensitivity of the percent of gas entering the structure to changes in (a) snow layer radius, (b) snow permeability; the dash-dot line corresponds to the simplified estimate discussed in the text, (c) annulus width, and (d) effective permeability of the annular region as a function of annulus width (inner radius: 9.53 mm); the default parameters were a snow radius of 1 m, a permeability of  $1.8 \times 10^{-9} \text{ m}^2$ , and an annulus width of 5 mm.

At large values of the snow radius, the amount entering the structure is linearly related to the log of the radius, and as the radius decreases the slope increases. Generally speaking, the effect of the snow radius is small relative to some other parameters, causing the amount to vary between 10% and 20% for the base case snow permeability, because most of the flow resistance occurs in the snow near the pipe.

The effect of the snow permeability is shown in Figure 6(b), for permeabilities in the range from  $1 \times 10^{-12}$  to  $1 \times 10^{-7} \text{ m}^2$  and annular gap widths of 5, 10, and 15 mm. This parameter clearly has a very large impact on what boundary is the most favorable for gas flow. Over the reported permeability range of snow ( $1 \times 10^{-10}$  to  $1 \times 10^{-8} \text{ m}^2$ ), the amount entering the structural gap (entering the structure) can be anywhere from several percent to 70% of the fugitive gas for an annular width of 5 mm. As the permeability decreases below  $1 \times 10^{-8} \text{ m}^2$ , the partitioning of the gas flow increasingly favors entering the structure due to the high flow resistance present in the snow layer. The dash-dot line without markers in Figure 6(b) corresponds to a simple estimate generated by comparing the flow through a snow cylinder to viscous flow in an annulus. The line was created by calculating the ratio:  $Q_{\text{an}}/(Q_{\text{an}} + Q_{\text{cyl}})$ , analogous to two flow resistances in parallel. The flow for these two simple systems can be calculated as velocity times the flow area (Equations (3) and (4)).

$$Q_{\text{cyl}} = \frac{k \cdot \Delta P}{\mu \cdot \ln\left(\frac{R_{\text{snow}}}{R_{\text{an}}}\right)} \cdot 2\pi R_{\text{snow}} \cdot L_{\text{total}} \quad (3)$$

$$Q_{\text{an}} = \frac{R_{\text{an}}^2}{8\mu} \frac{\Delta P}{\Delta L_{\text{leak}}} \left[ \frac{1 - \kappa^4}{1 - \kappa^2} - \frac{1 - \kappa^2}{\ln\left(\frac{1}{\kappa}\right)} \right] \cdot \pi(R_{\text{an}}^2 - R_{\text{pipe}}^2), \quad \text{where } \kappa \equiv \frac{R_i}{R_o} \quad (4)$$

For the cylinder, the pressure term was assumed to be  $\Delta P$  over 2 m of length and  $\frac{1}{2}\Delta P$  over 1 m of length, which is approximately correct when the snow permeability is low in the numerical simulations (resulting in constant pressure left of the leak and a linear decay toward the structure to the right of the leak). The annular flow was estimated by having a driving force of  $\Delta P$  over a length of 1 m. This simple approximation reproduces the calculations very well at low snow permeability, as would be expected based on the assumptions stated above. The same type of analysis can also be used to create a ‘scaled flow variable’ that will help to condense many of the numerical results into one curve, as discussed below.

The width of the annular region was determined to significantly affect the gas partitioning, and the results of the sensitivity analysis to this parameter are shown in Figure 6(c) for snow permeabilities of  $1 \times 10^{-10}$ ,  $1.8 \times 10^{-9}$ , and  $1 \times 10^{-8} \text{ m}^2$ . In the model, the effective permeability of the annular region also increases with the

annulus gap width in relation to viscous flow equations. As a result, the effective permeability of the annulus is highly dependent on the width. This dependence is shown in Figure 6(d) which shows that the permeability varies from approximately  $1 \times 10^{-7}$  to  $1 \times 10^{-4} \text{ m}^2$  over the range of widths examined. As the permeability of the gap approaches that of the snow, the lowest resistance path becomes the snow layer due to the much larger flow area.

As mentioned earlier, the gap permeability was calculated based on laminar flow in the annulus because of the linear equations that result. The flow in the gap will not be laminar over the entire range of velocities studied, so it is prudent to briefly discuss how this assumption may affect the results. For the base case with a gap width of 5 mm, the transition from the laminar regime will begin at axial velocities near 0.8 m/s. The effective permeability in the turbulent regime is dependent on the flow velocity and decreases as the velocity increases. For this particular case, an axial annular flow velocity of 0.8 m/s will result in a laminar effective permeability of approximately one-half of the turbulent effective permeability. The two will be equal at an axial velocity of approximately 1.5 m/s, and the laminar value will be approximately twice the turbulent value at a velocity of 3 m/s. Over the range of velocities expected to occur within the gap, the permeability values calculated for turbulent and laminar flow are within approximately a factor of 2.

Figure 7 shows all the data from Figure 6(a)–(c) as a function of the ‘scaled flow variable’ mentioned above. This independent variable is essentially the simple prediction of the fraction into the structure based upon the independent cylinder and annular flow approximations, and is defined as: ‘scaled flow variable’ =  $Q_{an}/(Q_{an} + Q_{cyl})$ . This new independent variable allows essentially all the results with varying snow layer thickness, snow permeability, and annulus thickness to fall on

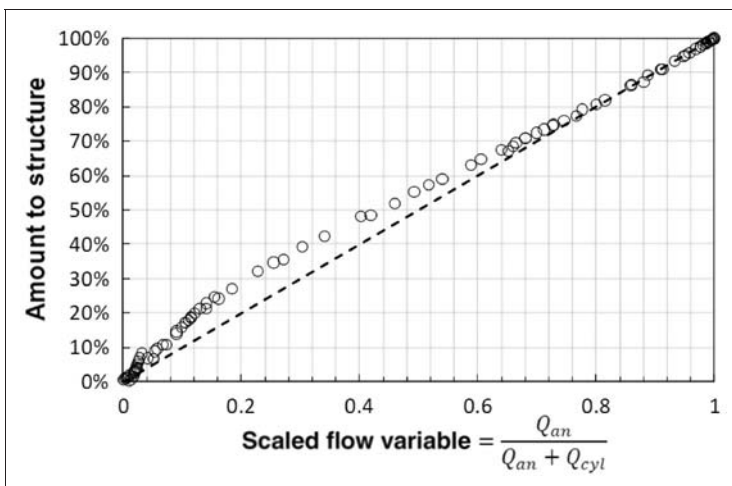


**Figure 7.** Numerical model results plotted as a function of a scale flow variable.

the same curve, confirming the fact that the main governing factor is the relative flow resistances of the annulus and the snow layers. If this simple approximation were exactly correct, all the data would fall on the 45° line shown in the figure. The data fall on the line at high values of the variable because these are typically the cases where a low snow permeability was used, allowing the assumptions made in calculating the variable to hold relatively well. When the fraction directed to the structure is low, the model deviates from the simple approximation. This is because the lower snow resistance allows more gas to escape through the snow, causing the assumptions that the pressure is constant left of the leak and that the pressure decay is linear right of the leak to no longer hold. Despite the deviations at small values of the scaled variable, the ability to condense most data onto a single curve may be useful when a detailed solution is not needed and only an estimate of the fraction entering a structure is required.

The effect of the location of the crack was investigated for a fixed total length of 3 m. Over the range 0.1–2.9 m from the structure, the amount entering the structure varies from approximately 80% to near zero for the base scenario snow permeability. The reason for this is that the pressure gradient driving annular flow decreases, and the further the leak is from the structural gap, the lower the velocity and flux will be through the gap. The rate of decay in the amount of gas to the structure as leak distance increases becomes more pronounced as the snow becomes more permeable.

The effect of the total length of the system, when the leak location is fixed at 1 m from the structure, is small. As the length of the system increases, more gas is allowed to escape through the snow due to increased surface area up to a critical length, over which increasing the length further does not affect the partitioning. The primary reason is that the pressure decreases rapidly as the distance from the leak location grows. This means that despite a longer length providing more surface area, the velocities far from source are small and the additional area makes little difference. This is a similar argument as to why the location of the leak makes such a large difference in what boundary is the preferred flow path for gas.

The effect of leak flow rate was examined by varying the flow rate between 0.0001 and 0.005 m<sup>3</sup>/s. The amounts exiting through the structural gap and the maximum relative pressures were between 17.1% and 0.25 Pa at the low flow rate and 17.1% and 12.7 Pa at the high flow rate. The leak rate clearly has a large impact on the pressure within the system, but does not significantly affect the distribution of gas flow. The calculations do not account for any mechanical work performed on the snow by gas impingement, and at high gas velocities this could be an important factor in the behavior of the system. Additionally, the calculations do not account for turbulent flow near the leak. The sublimation rate of the ice is also a potentially significant transient effect that will be discussed briefly in a later section.

One aspect this model does not take into account is the pressure drop from the outside edge of the wall to the inside of the structure; this is implicitly assumed to be zero. The details of the pressure drop will depend upon the nature of the gap.

To help quantify the potential pressure drop, annular viscous flow equations were used to estimate the pressure drop based upon the velocity at the exit of the calculation domain and assuming the structural gap is a perfect annulus of a given width. As before, the inner radius was assumed to 9.53 mm. The base scenario was used with structural gaps of both 2 and 1 mm, with corresponding average velocities at the structural gap of 2.6 and 5.5 m/s respectively. For the 2 mm gap, the pressure drop per unit length was calculated to be approximately 60 Pa/m and the pressure drop in the 1 mm gap was determined to be approximately 500 Pa/m.

The parameters examined in this section have varying degrees of impact on the gas partitioning, from relatively minor to major. The snow permeability, annular width, snow layer thickness, and location of the leak can all greatly affect the amount of gas that is directed into the structure. The internal pressure of the structure, or the pressure boundary condition at the structural gap, is also an important parameter that can greatly affect the partitioning of the gas flow and is discussed in the following section.

***Influence of the stack effect.*** The stack effect in a structure is the creation of a vertical pressure gradient due to heating of the interior above the ambient temperature. This creates a chimney-like effect where cold air is drawn in at the base of the structure and expelled near the top [16]. This can be a complex situation that is affected by the location of leak points, mechanical ventilation, wind impingement on the structure, and the internal temperature profile. However, evaluating a basic equation [16] for an external temperature of 273 K, an internal temperature of 293 K, an air density of  $1.29 \text{ kg/m}^3$ , and a structure height of 10 m results in a  $\Delta P_{\text{stack}}$  of  $-9.3 \text{ Pa}$ . Assuming the neutral pressure line at the center of the structure means that the internal pressure will be approximately 4.6 Pa below ambient at the base and 4.6 Pa above ambient at the top. To take this effect into account, the model results can be examined when the internal pressure is several Pascals below the ambient pressure at the snow surface.

When the pressure at the structural gap is below the ambient pressure, it opens up the possibility for air flow from the ambient, through the snow, and into the structure. This is manifested in a negative radial velocity at the snow surface. When calculating the amount of the fugitive gas entering the structure, simply summing the fluxes at the leak, snow surface, and through the gap can yield percentages above 100% due to more air entering through the snow surface than gas flow out of the snow. Therefore, when computing the flux of fugitive gas through the snow, positive radial velocities are treated as fugitive gas flow out and negative radial velocities are treated as air flow in. The air flow portion of the flux is ignored when computing the fraction of fugitive gas exiting through the structural gap. This calculation assumes that fugitive gas that leaves through the snow surface is lost and is not reintroduced to the system through entrainment in the air entering the snow.

The effect of the pressure difference is shown in Figure 8(a) and (b), with Figure 8(a) showing both the total flow into the structure (including entrained



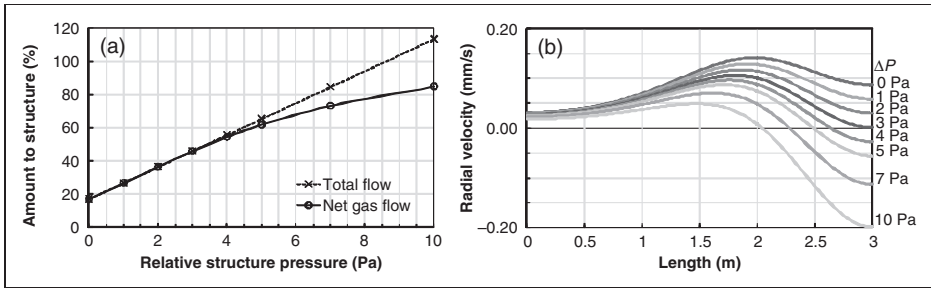


**Figure 8.** (a) Effect of relative structure pressure ( $\Delta P = P_{amb} - P_{int}$ ) on the fraction of gas entering the structure; (o) ‘net gas flow’ ignores air flow into the system when computing partitioning and will approach an asymptote at 100%, (x) ‘total flow’ includes entrained air when computing the amount to the structure and will continue to rise as the pressure difference increases; (b) effect of relative structure pressure on the radial velocity at the snow surface.

air) and the net gas flow into the structure, as discussed above. Figure 8(b) shows the effect of the pressure differential on the radial velocity at the snow surface. Below pressure differentials of 3 Pa, the radial velocity is always positive, so no air enters the system from the ambient. At larger  $\Delta P$  values, the velocity at the snow surface near the structural gap turns negative and the magnitude becomes larger as the pressure differential grows. The relative pressure for which the radial velocity is negative (flow into the system) over the entire length for this set of conditions was determined to be approximately 25 Pa (0.1 in. of water), at which point 100% of the fugitive gas would exit through the structural gap with a significant amount of entrained air. This would correspond to an unrealistic temperature differential for a 10-m tall building, assuming no effect from the wind. However, the pressure inside the structure is clearly a potentially important factor to consider when performing an analysis, as pressure differences of several Pascals can drastically change the partitioning of the gas flow.

The pressure field for the scenario when the internal structural pressure is 4 Pa below the ambient pressure is shown in Figure 9(a). The ambient pressure contour is shown as a bold line in the figure, indicating that the domain pressures to the left of the bold contour are above ambient pressure and those to right are below ambient pressure. This means that the radial velocities at the snow surface and to the right of the bold contour will be negative (into the domain), which agrees with the radial velocity results shown in Figure 8. The lines in Figure 9(b) show the contours of ambient pressure for the range of pressure differentials between 1 and 28 Pa. As the pressure of the structure decreases (larger  $\Delta P$ ), the ambient pressure contour moves away from the structure indicating the larger field of sub-ambient pressures present near the structure. The length over which the radial velocity is directed into the domain also increases from zero at low pressure differentials to 100% above 25 Pa. In this figure, the top boundary is always at ambient pressure.

The stack effect in the structure and the resulting internal pressure gradient can greatly affect whether the gas flows into the ambient environment or into the

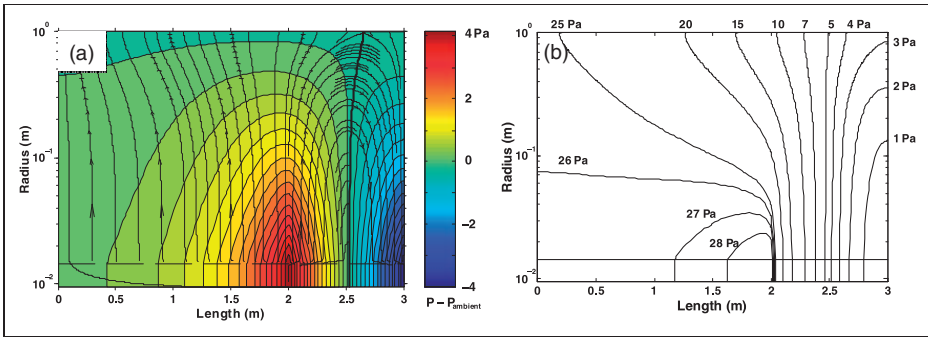


**Figure 9.** (a) Pressure field when the structure pressure is 4 Pa below the ambient pressure; the bold line is the ambient pressure contour; (b) location of ambient pressure contour lines for a range of pressure differentials.

structure. Pressure differentials of several Pascals between the internal and ambient pressures can cause large swings in the amount of gas entering the structure. It is certainly possible to have pressure differentials of this magnitude generated by the stack effect in a normal building. Mechanical ventilation or wind effects can create additional pressure differentials.

**Effect of a surface ice layer.** Another physical phenomenon that can significantly affect the partitioning of the fugitive gas is the formation of an ice layer on top of, or within, the bulk snow. Snow often forms a crust or ice layer on top of a lower density bulk layer. The formation of such an ice layer can occur through several mechanisms, including melting/refreezing of the top layer of snow and freezing rain being deposited on top of the bulk snow. This phenomenon was observed in the snow test performed in late January in which a snow fall was followed by approximately 12 mm of sleet and by another 5 mm of sleet and freezing rain. The result was a mostly solid top layer of ice on the order of 5 mm thick. As mentioned earlier, the top layer of sleet/ice had a density of over  $600 \text{ kg/m}^3$ ; the density of pure ice is approximately  $920 \text{ kg/m}^3$ . If ice is present on top of the snow (or at some intermediate level within the snow layer but above the leak location), it will serve as another high-resistance layer that resists the flow of gas into the ambient, allowing more fugitive gas to be directed into the structure.

The model was adjusted so that another layer of a specified permeability could be added on top of the snow layer to mimic the conditions after the formation of an ice layer. The thickness and permeability of the ice layer could be varied to determine the effect of the parameters on the system behavior. In these calculations, the parameters of the base model were used unless otherwise specified. The thin ice layer was modeled with a dense set of grid points to ensure accurate calculation of the flux in and out of the region.

Previous publications [17] indicate that natural ice layers taken from the field have permeability values that range from  $5 \times 10^{-13}$  to  $1 \times 10^{-9} \text{ m}^2$  based on

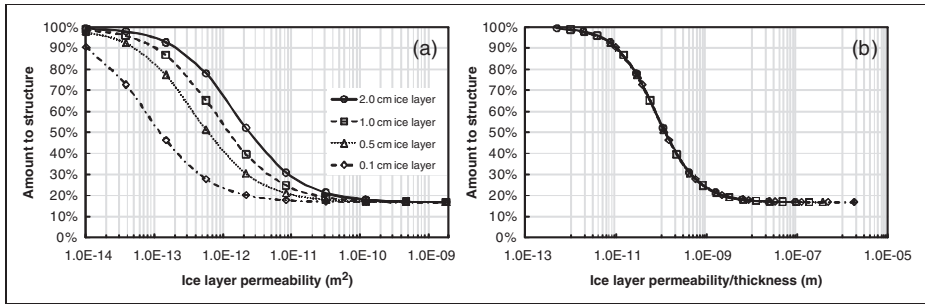


**Figure 10.** Effect of (a) ice layer permeability and (b) thickness on the partitioning of the fugitive gas; snow layer permeability:  $1.8 \times 10^{-9} \text{ m}^2$ .

samples from Canada. Another study [15] measured the permeability of ice layers found within a snow pack in Vermont, and determined that the ice permeability was in the range  $1 \times 10^{-10}$  to  $2 \times 10^{-9} \text{ m}^2$ . A recent study of the permeability of lake ice in Antarctica [18] has determined that permeability values typically fall in the range  $10^{-14}$  to  $10^{-13} \text{ m}^2$ , with an average value of approximately  $1 \times 10^{-13} \text{ m}^2$ . Although lake ice may not be wholly representative of ice layers formed by melting/refreezing snow or freezing rain, properties of lake ice are considered to provide a lower bound on permeability for the parametric analysis. Based on these sources, reasonable values for the permeability of ice can be bounded by the solid ice value of  $1 \times 10^{-13} \text{ m}^2$  and the real-world ice layers measured at  $1 \times 10^{-9} \text{ m}^2$  that would account for heterogeneities and defects.

The effect of ice layer permeability on the amount of fugitive gas entering the structure is shown in Figure 10(a) for four ice layer thicknesses. The gas partitioning clearly depends on both thickness and permeability, but only because these two parameters determine the overall resistance of the layer to gas flow. If the data are plotted as a function of permeability divided by ice layer thickness, then all data lie on the same curve, as shown in Figure 10(b) demonstrating that the effect can be modeled as an effective resistance.

The relative values of the snow and ice layer permeability will affect the partitioning of the fugitive gas. The effect of both layers is shown in Figure 11(a) for a snow layer thickness of 1 m and an ice layer thickness of 5 mm. As expected, if either of the layers has a very low permeability, then essentially all the gases are directed into the structure, and if both the layers have a very high permeability almost no gas enters the structure. It is interesting to note that for a given ice permeability, the minimal amount of gas entering the building occurs at an intermediate snow permeability. Specifically looking at low values of ice permeability, the fraction of gas entering the building approaches 1 at both low and high snow permeabilities. The increased fraction directed to the structure at higher snow permeability occurs because the snow acts like a very large annulus, reducing the overall pressure in the snow region and reducing the driving force for gas flow through the ice layer. This allows more gas to enter the structure.

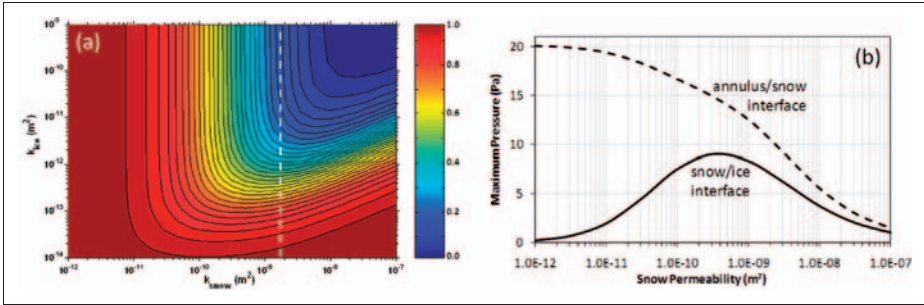


**Figure 11.** (a) Fraction of gas entering the structure as a function of snow and ice permeability for an ice layer thickness of 5 mm and a snow layer thick of 1 m; the dashed line shows the base model snow permeability; (b) maximum pressure at the annulus/snow interface and the snow/ice interface as a function of snow layer permeability for an ice layer permeability of  $1 \times 10^{-13} m^2$ .

The maximum pressures along the annulus/snow and snow/ice interfaces as a function of snow permeability are shown in Figure 11(b) for an ice permeability of  $1 \times 10^{-13} m^2$ . It is clear from this that the fraction to the structure is highly dependent on the maximum pressure developed at the edge of the ice domain. At low snow permeabilities, the snow/ice interface pressure is low because the majority of the pressure drop occurs in the snow layer. At high snow permeability, the driving force for flow through the ice layer is low because the pressure is low throughout the snow region due to small pressure gradients needed to drive flow in the low-resistance snow layer.

For very high permeability snow, most of the gas is able to flow out of the structural gap, even after traveling very near to the ice layer. The combination of highly permeable snow with a thick, low permeability ice layer may pose the greatest hazard, because the fugitive gas is relatively free to flow in the snow layer and may find entry points to the structure not associated with the gap around the gas piping. This is especially true where the snow layer is confined by walls or natural containment from sloping ground, as in the numerical simulations with the impermeable left-hand boundary.

**Effect of sublimation.** Sublimation, evaporation of snow or ice, can play an important role in the partitioning of gas between the ambient and the structure by increasing the size of any gaps along the leak path. This is because the gas leaking from the pipe should be dry, creating a large driving force for the stripping of water vapor from ice crystals along the flow path. As the gas flow continues, this would have the effect of decreasing the flow resistance by increasing the area available for flow. The width of the annular region would increase as ice is converted into water vapor and carried away by the gas flow, and the density of the snow layer in the vicinity of the leak would decrease through the same mechanism. To get

an estimate of the rate of ice sublimation due to gas flow, a simple mass-transfer problem can be solved for a dry gas flow in a solid 'snow tube' with a wall roughness approximately equivalent to the snow grain size.

Based upon the simple estimation scheme, the calculated rate of ice loss per centimeter of length was determined to be between 0.2 g/h at the beginning of the tube to 0.023 g/h after 1.0 m of length. Regions nearest the leak would be removed by sublimation first, while regions further away from the leak would have a lower rate of removal as the concentration of water in the bulk gas approaches its equilibrium value. Over the entire 1 m length of tube, sublimation results in an initial ice loss rate of approximately 8.3 g/h or 40 mL/h. This means that the annular volume would increase by approximately 10% in the first hour over the 1 m length if the flux remained constant. It is clear from this simple estimate that sublimation could significantly increase the annular gap width and change the amount of gas that is directed into the structure.

## Conclusions

The combination of observations from the experimental investigation and the numerical results from the modeling exercise shows that plausible conditions exist that can lead to a significant amount of fugitive gas entering a structure from a leak in a nearby snow-covered pipe. However, natural variability in important parameters can greatly change the preferred pathway for gas migration, and whether gas is preferentially funneled into a structure will depend upon the details of the situation. The pressure inside of the structure at the entry point was found to be perhaps the most influential parameter, with the ability to draw a large portion of the flow into the structure if the internal pressure is several Pascals below the ambient pressure. The distance of the leak point from the structural gap was another parameter with a major impact on the gas distribution. Leaks close to the structure result in more gas entering the structure than leaks farther from the structure. Snow permeability can also greatly affect the results, and over the natural range of permeability values, the amount of gas entering the structure can significantly vary. The history and aging of the snow layer can play a major role because the time and temperature history both affect the snow layer density, permeability, and potentially the size of the void space beneath the pipe. The size of the annular region and the thickness of the snow layer also played a role, with the results being more sensitive to the annular gap width. The formation of a low-permeability ice layer is also an important phenomenon that can drastically change the behavior of the system, but depends heavily on the ice layer permeability. The effect of ice crystal sublimation has the ability to significantly change the geometry of the annular region over relatively short times, potentially allowing for the amount of gas entering the structure over time to increase as the annular gap widens. Whether this enhancement occurs will depend on the competitive reductions in the flow resistance in the snow layer and the annulus due to the loss of ice.

## Acknowledgments

The authors thank Exponent, Inc. for generous support for this study and the Snows for use of the property where the snow tests were performed.

## Endnote

a. Based on analysis of fire department reports, news articles, and other reports.

## References

1. NFPA. *NFPA 58 – Liquefied Petroleum Gas Code*. Section 6.13: Installation in areas of heavy snowfall. Quincy, MA, USA: National Fire Protection Association, 2004.
2. US Army Corp of Engineers. *Technical instructions: commentary on snow loads*. TI 809-52. Washington, DC: US Army Corp of Engineers, 1998.
3. NFPA. *NFPA 921: Guide for fire and explosion investigations*. Sections 9.9.7 and 21.8.3: Underground migration of fuel gases. Quincy, MA, USA: National Fire Protection Association, 2004.
4. Jacobus J and Yaeger AG. Gas leak migration: reports detail unusual patterns in some gas leak incidents. *Pipeline & Gas Journal* October 2007; 38–43.
5. Albert MR and Shultz EF. Snow and firn properties and air-snow transport processes at summit, Greenland. *Atmospheric Environment* 2002; Vol. 36: 2789–2797.
6. Albert MR. Modeling heat, mass, and species transport in polar firn. *Annals of Glaciology* 1996; Vol. 23: 138–143.
7. Jordan RE, Albert RM and Brun E. Physical processes within the snow cover and their parameterization. In: Armstrong Richard, Brun Eric (eds) *Snow and climate: physical processes, surface energy exchange and modeling*. Cambridge, UK: Cambridge University Press, 2008.
8. Kaempfer TU and Schneedeli M. Observation of isothermal metamorphism of new snow and interpretation as a sintering process. *Journal of Geophysical Research* 2007; Vol. 112: D24101.
9. Coleou C, Pieritz RA, Lesaffre B, Brzoska JB and Etchevers P. Isothermal metamorphism of a new snow layer: some measurements and simulation. In: *International snow science workshop 2004 Proceedings*, Jackson Hole, Wyoming.
10. Bird RB, Stewart WE and Lightfoot EN. *Transport phenomena*. Somerset, NJ: John Wiley & Sons, 1960.
11. Geankoplis CJ. *Transport processes and unit operation*, 3rd edn. Englewood Cliffs, NJ: Prentice Hall, 1993.
12. Shimizu H. Air permeability of deposited snow. *Contributions from the Institute of Low Temperature Science* 1970; Vol. A22: 1–32.
13. Bender JA. Air permeability of snow. Research Report, Vol. 37, US Army Corps of Engineers, Snow, Ice and Permafrost Research, 1957.
14. Hardy JP and Albert DG. The permeability of temperate snow: preliminary links to microstructure. In: *50th Eastern Snow Conference/61st Western Snow Conference*, Quebec City, 1993.
15. Albert MR and Perron FE. Ice layer and surface crust permeability in a seasonal snow pack. *Hydrological Processes* 2000; Vol. 14: 3207–3214.
16. ASHRAE. *ASHRAE handbook: fundamentals*. Atlanta, GA: American Society of Heating, Refrigeration, and Air-Conditioning Engineers, Inc, 2005.

- 
17. Fortin G, van Bochove E, Jones HG, Thériault G and Bernier M. The simultaneous determination of air permeability and gas diffusion through ice layers in the field. *Nordic Hydrology* 2007; Vol. 38: 203–210.
  18. Carroll KP. Permeability of lake ice in the Taylor Valley, Antarctica: from parameter design to permeability upscaling. Master's Thesis, Columbus, USA, The Ohio State University, 2008.